Fish & Shellfish Immunology 33 (2012) 99–110

Contents lists available at SciVerse ScienceDirect

Fish & Shellfish Immunology

journal homepage: www.elsevier.com/locate/fsi

Caspase 3 from rock bream (*Oplegnathus fasciatus*): Genomic characterization and transcriptional profiling upon bacterial and viral inductions

Don Anushka Sandaruwan Elvitigala [a,1], Ilson Whang [a,1], H.K.A. Premachandra [a], Navaneethaiyer Umasuthan [a], Myung-Joo Oh [b], Sung-Ju Jung [b], Sang-Yeob Yeo [c], Bong-Soo Lim [d], Jeong-Ho Lee [e], Hae-Chul Park [f,**], Jehee Lee [a,d,*]

[a] *Department of Marine Life Sciences, School of Marine Biomedical Sciences, Jeju National University, Jeju Self-Governing Province 690-756, Republic of Korea*
[b] *Department of Aqualife Medicine, Chonnam National University, Chonnam 550-749, Republic of Korea*
[c] *Department of Biotechnology, Division of Applied Chemistry & Biotechnology, Hanbat National University, Daejeon 305-719, Republic of Korea*
[d] *Marine and Environmental Institute, Jeju National University, Jeju Special Self-Governing Province 690-814, Republic of Korea*
[e] *Genetics & Breeding Research Center, National Fisheries Research & Development Institute, Geoje 656-842, Republic of Korea*
[f] *Graduate School of Medicine, Korea University, Ansan, Gyeonggido 425-707, Republic of Korea*

ARTICLE INFO

Article history:
Received 26 January 2012
Received in revised form
31 March 2012
Accepted 16 April 2012
Available online 21 April 2012

Keywords:
Caspase 3
Rock bream
Recombinant protein
Hydrolyzing activity
Transcriptional analysis

ABSTRACT

Caspase 3 is a prominent mediator of apoptosis and participates in the cell death signaling cascade. In this study, caspase 3 was identified (*Rbcasp3*) and characterized from rock bream (*Oplegnathus fasciatus*). The full-length cDNA of *Rbcasp3* is 2683 bp and contains an open reading frame of 849 bp, which encodes a 283 amino acid protein with a calculated molecular mass of 31.2 kDa and isoelectric point of 6.31. The amino acid sequence resembles the conventional caspase 3 domain architecture, including crucial amino acid residues in the catalytic site and binding pocket. The genomic length of *Rbcasp3* is 7529 bp, and encompasses six exons interrupted by five introns. Phylogenetic analysis affirmed that Rbcasp3 represents a complex group in fish that has been shaped by gene duplication and diversification. Many putative transcription factor binding sites were identified in the predicted promoter region of Rbcasp3, including immune factor- and cancer signal-inducible sites. Rbcasp3, excluding the pro-domain, was expressed in *Escherichia coli*. The recombinant protein showed a detectable activity against the mammalian caspase 3/7-specific substrate DEVD-*p*NA, indicating a functional role in physiology. Quantitative real time PCR assay detected Rbcasp3 expression in all examined tissues, but with high abundance in blood, liver and brain. Transcriptional profiling of rock bream liver tissue revealed that challenge with lipopolysaccharides (LPS) caused prolonged up-regulation of *Rbcasp3* mRNA whereas, *Edwardsiella tarda* (*E. tarda*) stimulated a late-phase significant transcriptional response. Rock bream iridovirus (RBIV) up-regulated Rbcasp3 transcription significantly at late-phase, however polyinosinic-polycytidylic acid (poly(I:C)) induced Rbcasp3 significantly at early-phase. Our findings suggest that Rbcasp3 functions as a cysteine-aspartate-specific protease and contributes to immune responses against bacterial and viral infections.

1. Introduction

Apoptosis, one of the biochemically classified programmed cell death types, is a highly regulated process in multicellular organisms that is triggered by external and internal stimuli [1–3]. Apoptosis can play a significant role in cellular immunity, acting as an immune response to infections, especially those related to viruses [4,5]. The primary regulators of apoptosis are the host-encoded caspases [6–8]. Caspases are an evolutionarily conserved family of **c**ysteine-**a**spartic **s**pecific **p**rote**ase**s responsible for a diverse array of cellular functions, the well-recognized of which are apoptosis and inflammation. In pre-apoptotic cells, caspases

* Corresponding author. Marine Molecular Genetics Lab, Department of Marine Life Sciences, College of Ocean Science, Jeju National University, 66 Jejudaehakno, Ara-Dong, Jeju 690-756, Republic of Korea. Tel.: +82 64 754 3472; fax: +82 64 756 3493.
** Corresponding author. Graduate School of Medicine, Korean University, Ansan, Gyeonggido 425-707, Republic of Korea. Tel.: +82 31 412 6712; fax: +82 31 412 6729.
E-mail addresses: hcpark67@korea.ac.kr (H.-C. Park), jehee@jejunu.ac.kr, jeheedaum@hanmail.net (J. Lee).
[1] These authors contributed equally to this work.

1050-4648/$ – see front matter © 2012 Elsevier Ltd. All rights reserved.
doi:10.1016/j.fsi.2012.04.008

exist as inactive pro-enzymes (zymogenes) [9], which mainly consist of three distinct domains: a pro-domain, followed by a large subunit and a small subunit. The latter two subunits are connected by a linker region, which itself is flanked by aspartic acid residues [10].

Caspases can be self-activated or be activated by upstream-caspase proteases in death cascade that cleaves conserved aspartic acids in the C terminal region [11]. To date, 11 human caspases have been identified and functionally categorized into two groups; inflammatory caspases and apoptotic caspases. The latter has been further divided into initiators and effectors [8]. The effector caspases (caspase 1, 3, 4, 5, 6, 7, and 11) are activated by the self-activated initiator caspases, which function in the upstream of the apoptotic signaling pathway [12,13]. Caspases and caspase-like enzymes have also been identified in non-metazoans, such as plants, fungi, and prokaryotes [14]. Caspases are regulated at several stages, such as at the transcriptional and post-transcriptional levels [1]. Moreover, enzymatic activity of caspases can be inhibited by members of a conserved family of proteins known as inhibitor of apoptosis (IAP) factors [15].

Caspase 3, one of the effector caspases, is involved in executing the cell death signaling cascade of intrinsic and extrinsic apoptotic pathways, following its activation by caspase 8 and caspase 9, respectively [16]. Activated caspase 3 mediates many of the characteristic morphological alterations of apoptosis, such as breakdown of several cytoskeletal proteins, cleavage of polyadenosine dipeptide ribose polymerase (PARP) and degradation of the inhibitor of caspase-activated DNAses (ICADs), resulting in the release of CAD to cleave cell DNA and ultimately directing the cell toward death [7].

Caspase 3 has been identified and characterized in several teleost fish species; Studies of caspase 3 homologs in European sea bass (*Dicentrarchus labrax)*, zebrafish (*Danio rerio*), large yellow croaker (*Pseudosciaena crocea*), and Atlantic salmon (*Salmo salar*) have revealed an immune-related functions in these fishes [17–20]. Furthermore, two isoforms of caspase 3 (A and B) have been identified in Medaka (*Oryzias latipes*) [21] and Atlantic salmon [20].

Rock bream is one of the most economically important marine fish species in South Korea, which domiciliates in the coastal areas of the Pacific and Indian Ocean. In recent years, the mariculture sources of rock bream have experienced an alarming increase in prevalence and virulence of pathogenic infections, which have resulted in considerable economic losses [22,23]. Therefore, it is important to gain a detailed understanding of the unknown genetic and immunological mechanisms against pathogens in rock bream, in order to launch effective disease control interventions and disease-tolerant species by genetic breeding. In this study, we discovered and characterized the rock bream caspase 3 (*Rbcasp3*) at transcriptional and genomic levels. We determined the basal tissue distribution and transcriptional response in liver tissue to immune challenges with lipopolysaccharide (LPS), *Edwardsiella tarda*, rock bream iridovirus (RBIV), and polyinosinic-polycytidylic acid (poly (I:C)). We not only demonstrated that Rbcasp3 harbors immune-related hydrolytic activity using recombinant protein, but also determined that apoptosis represents an immune responsive process in rock bream.

2. Materials and methods

2.1. Identification of full-length cDNA sequence of Rbcasp3

Using the Basic Local Alignment Tool (BLAST) algorithm (http://www.ncbi.nlm.nih.gov/BLAST), full-length cDNA sequence of caspase 3 (contig number-07658) in -rock bream was identified from a previously established cDNA sequence data base [24].

2.2. Rbcasp3 genomic BAC library construction and PCR screening

Using rock bream genomic DNA, a random sheared bacterial artificial chromosome (BAC) library was custom constructed (Lucigen, USA). The library was screened by PCR in order to identify the clone containing the full-length Rbcasp3 gene using a sequence specific primer pair Rbcasp3-qF and Rbcasp3-qR (Table 1), designed according to the identified *Rbcasp3* cDNA sequence. The identified BAC clone was sequenced by GS-FLX™ system (Life Sciences, USA).

2.3. In silico analysis of rock bream caspase 3 DNA and protein sequences

The orthologous sequences of *Rbcasp3* were compared by the BLAST search program. Pairwise sequence alignment (http://www.Ebi.ac.uk/Tools/emboss/align) and multiple sequence alignment (http://www.Ebi.ac.uk/Tools/clustalw2) were performed using the ClustalW2 program. The phylogenetic relationship of *Rbcasp3* was determined using the Neighbor-Joining method and Molecular Evolutionary Genetics Analysis (MEGA) software version 4 [25]. Prediction of protein domains was carried out using the ExPASy-prosite data base (http://prosite.expasy.org) and the MotifScan scanning algorithm (http://myhits.isb-sib.ch/cgi-bin/motif_scan). Some properties of Rbcasp3 were determined by ExPASy Prot-Param tool (http://web.expasy.org/protparam).

Genomic sequence of *Rbcasp3* obtained from the BAC clone was used to identify the exon–intron structure and predict the promoter region along with potential transcriptional factor binding sites. The transcription initiation site (TIS) was predicted using the online neural network promoter prediction tool from Berkeley Drosophila Genome Project [26]. Potential cis acting elements located ~1 Kb upstream of the TIS were detected using TFSEARCH ver.1.3 and Alibaba 2.1 software. Furthermore, the tertiary structure of Rbcasp3 pro-enzyme was modeled based on the ab-initio protein prediction strategy, using the online server I-TASSER [27,28]. Subsequently, the three dimensional (3D) image was generated utilizing RasMol 2.7.5.2 software.

Table 1
Primers used in this study. F and R refer to forward and reverse primers, respectively. The lowercase letters indicate restriction enzyme sites introduced for cloning.

Name	Purpose	Sequence (5′ → 3′)
Rbcasp3-F	ORF amplification (without pro- domain)	GAGAGAgaattcGCCAAGCCCAGCTCCCACAG
Rbcasp3-R	ORF amplification (without pro-domain)	GAGAGActgcagTCAAGGAGAAAAATACATCTCTTTGGTCAGCATTG
Rbcasp3-qF	qRT-PCR primer	TGAGGGTGTGTTCTTTGGTACGGA
Rbcasp3-qR	qRT-PCR primer	TTCCCACTAGTGACTTGCAGCGAT
Rb-β-actin-F	qRT PCR internal reference	TCATCACCATCGGCAATGAGAGGT
Rb-β-actin-R	qRT PCR internal reference	TGATGCTGTTGTAGGTGGTCTCGT

2.4. Expression and purification of recombinant Rbcasp3 (rRbcasp3)

Recombinant Rbcasp3, excluding the pro-domain, was expressed as a fusion protein with Maltose Binding Protein (MBP) and purified as described previously with some modifications [29]. Briefly, the Rbcasp3 gene encoding residues 33–283 was amplified using the sequence specific primers Rbcasp3-F and Rbcasp3-R with restriction enzyme sites for *Eco*RI and *Pst*I respectively (Table 1). The PCR was performed in a TaKaRa thermal cycler in a total volume of 50 μL with 5 U of Ex*Taq* polymerase (TaKaRa, Japan), 5 μL of 10x Ex *Taq* buffer, 8 μL of 2.5 mM dNTPs, 80 ng of template, and 20 pmol of each primer. The reaction was carried out at 94 °C for 30 s, 55 °C for 30 s, 72 °C for 1 min and final extension at 72 °C for 5 min. The PCR product (~753 bp) was resolved on a 1% agarose gel, excised and purified using the Accuprep™ gel purification kit (Bioneer Co. Korea). The digested pMAL-c2X vector (35 ng) and PCR product (15 ng) were ligated using Mighty Mix (7.5 μl; TaKaRa) at 4 °C overnight. The ligated pMAL-c2X/Rbcasp3 product was transformed into DH5α cells and sequenced. Sequence confirmed recombinant expression plasmid was transformed into *Escherichia coli* BL21 (DE3) competent cells. The recombinant Rbcasp3 protein was overexpressed using isopropyl-β-galactopyranoside (IPTG, 1 mM final concentration) at 37 °C for 3 h, after which the protein was purified using pMAL protein fusion and purification system (New England Biolabs, USA). The purified protein was eluted with elution buffer (10 mM maltose) and the concentration was determined by the Bradford method using bovine serum albumin (BSA) as the standard [30]. The Rbcasp 3 samples collected from different purification steps were analyzed on 12% SDS-PAGE under reduced conditions, with standard protein size marker (TaKaRa). The gel was stained with 0.05% Coomassie blue R-250, followed by a standard destaining procedure.

2.5. Hydrolyzing activity assay of rRbcasp3

With the objective of characterizing the purified rRbcasp3, hydrolyzing activity was analyzed by using caspase 3 activity assay kit (BioVision, USA) following manufacturer's protocol. Briefly, the purified protein was adjusted to 2 μg/μL and 50 μL was mixed with 50 μL 2x reaction buffer and 5 μL of 4 mM caspase 3/7 specific substrate (DEVD-*p*NA), followed by incubation at 37 °C for 2 h. The cleavage and release of *p*NA was measured by monitoring absorbance at 400 nm using a spectrophotometer. In order to assess the specificity of Rbcasp 3 against DEVD-*p*NA, its activity against caspase 9 and caspase 8 substrates (LEHD-*p*NA and IETD-*p*NA, respectively from Bio Vision USA) was also analyzed. Each assay was conducted with the MBP control, to determine the effect of fusion protein on the activity of rRbcasp3. All the assays were carried out with three replicates. The mean absorbance values obtained in the assay for both fusion protein and MBP alone were expressed to represent the hydrolyzing activities.

2.6. Experimental fish and tissue collection

Rock bream with an average body weight of 30 g were obtained from the Jeju Special Self-Governing Province Ocean and Fisheries Research Institute (Jeju, Republic of Korea). The fish were maintained in a controlled environment at 22–24 °C. All individuals were allowed to acclimate for one week prior to experimentation. Whole blood (1 mL/fish) was collected from the caudal fin using a sterilized syringe, and the sample was immediately centrifuged at 3000 × g for 10 min at 4 °C to separate the blood cells from the plasma. The collected cells were snap-frozen in liquid nitrogen. Meanwhile, the sampled fish was sacrificed and the gill, liver, skin, spleen, head kidney, kidney, skin, muscle, brain and intestine were excised and immediately snap-frozen in liquid nitrogen and stored at −80 °C until use for total RNA extraction.

2.7. Immune challenge experiments

In order to determine the immune responses of *Rbcasp3*, *E. tarda*, RBIV, LPS and the viral dsRNA mimic poly(I:C) were employed as immune stimulants in time course experiments. Tissues were collected as described in Section 2.6. The immune challenge experiments were carried out as described previously, sacrificing three animals for the tissue collection from each challenge group at each time point [31].

2.8. Total RNA extraction and cDNA synthesis

Total RNA was extracted from each of the excised tissues by using the Tri Reagent™ (Sigma–Aldrich, USA). Concentration of RNA was determined at 260 nm in a UV-spectrophotometer (Bio-Rad, USA) and diluted to 1 μg/μL 2.5 μg of RNA from selected tissues was applied in cDNA synthesis using cDNA synthesis kit (TaKaRa, Japan) according to the manufacturer's instructions. Finally, the newly synthesized cDNA was diluted 40-fold (total 800 μl) and stored at −20 °C until needed for further analysis.

2.9. Rbcasp3 mRNA expression analysis by quantitative real time (qRT-) PCR

qRT-PCR was used to detect the expression levels of Rbcasp3 in blood, gill, liver, spleen, head kidney, kidney, skin, muscle, brain and intestine tissues, and the temporal expression of Rbcasp3 in liver. Total RNA was extracted at different time points following immune challenge, and the first-strand cDNA synthesis was carried out as described in Section 2.8. qRT-PCR was carried out using the thermal cycler Dice™ Real Time System (TP800; TaKaRa, Japan) in a 15 μL reaction volume containing 4 μl of diluted cDNA from each tissue, 10 μL of 2x TaKaRa Ex Taq™, SYBR premix, 0.5 μL of each primer (Rbcasp3-qF and Rbcasp3-qR; Table 1), and 5 μL of ddH_2O. The qRT-PCR was performed under the following conditions: 95 °C for 10 s, followed by 35 cycles of 95 °C for 5 s, 58 °C for 10 s and 72 °C for 20 s and a final cycle of 95 °C for 15 s, 60 °C for 30 s and 95 °C for 15 s. The base line was set automatically by Dice™ Real Time System software (version 2.00). Rbcasp3 expression was determined by the Livak ($2^{-\Delta\Delta CT}$) method [32]. The same qRT-PCR cycle profile was used for the internal control gene, rock bream β-actin (Genbank ID: FJ975146). All data are presented as means ± standard deviation (SD) of relative mRNA expression of triplicates. To determine statistical significance ($P < 0.05$) between the experimental and control groups, the two-tailed paired *t*-test was carried out.

3. Results

3.1. Molecular characterization and phylogenetic analysis of Rbcasp3

The full-length sequence of *Rbcasp3* consists of 2756 nucleotides (nt), which is comprised of a 849 bp open reading frame (ORF) encoding 283 amino acids, a 159 bp 5′ untranslated region (5′ -UTR), and a 1748 bp 3′ -UTR. The 3′ -UTR contains a polyadenylation signal (^{2730}AATAAA^{2735}) and three RNA instability motifs (^{2027}ATTTA^{2031}, ^{2205}ATTTA^{2209}, ^{2592}ATTTA^{2596}) (Fig. 1). Moreover, the predicted molecular mass of Rbcasp3 was around 31.2 kDa and the theoretical isoelectric point was 6.31.

Resembling the typical caspase domain architecture, Rbcasp3 contained a putative pro-domain (residues 1–36), a large subunit

Fig. 1. Nucleotide and deduced amino acid sequence of Rbcasp3. The start codon (ATG), the stop codon (TGA), and the polyadenylation signal sequence (ATTAAA) are indicated by gray shading. The protein binding domain (GSWFI) and the penta-peptide active site motif (QACRG) are depicted in boxes. Three RNA instability motifs (ATTTA) are shown by underling.

(residues 52–176), and a small subunit (residues 189–283) as predicted by ExPASy PROSITE server. Several amino acid residues that are known to be critical for the function of caspase 3 catalytic center (Cys^{172}, His^{130}, Gly^{131}) and binding pocket (Gln^{170}, Arg^{244}, Ser^{257}) were found to be well conserved in Rbcasp3 [19]. Moreover, the characteristic active site penta-peptide motif (^{170}QACRG^{174}) was also identified in the large subunit of Rbcasp3. The protein binding domain ^{218}GSWFI^{222} [33] present within the small subunit also exhibited a significant conservation among the species analyzed with only a conservative substitution in the last amino acid of the motif for Atlantic salmon, large yellow croaker, and fugu (*Takifugu rubripes*) (Fig. 2). Similarly, the integrin recognition motif (^{152}RGD^{154}) [34] in Rbcasp3 near the active site was found to be conserved in all species analyzed, with the exceptions of sea bass caspases 3 and Medaka caspases 3A variant, wherein the aspartate residue is replaced by an asparagine in sea bass and arginine and aspartate residues are replaced by lysine and arginine residues respectively in Medaka (Fig. 2).

Multiple sequence alignment revealed that Rbcasp3 has significant identity with vertebrate orthologues; for instance, caspase 3 homologs in large yellow croaker and human shared 88.8% and 54.1% of identity with Rbcasp3, respectively. In contrast, Rbcasp3 from invertebrates showed lower identity; for example, that of black tiger shrimp shared only ~28% identity with Rbcasp3 (Table 2). Phylogenetic analysis was carried out using the Neighbor-Joining method to compare Rbcasp3 sequence with different vertebrate and invertebrate caspase 3 members (Fig. 3). The tree revealed that Rbcasp3 forms a clade with the caspase 3 of large yellow croaker, exhibiting a fairly high bootstrap supporting value (74). Moreover, this analysis confirmed that Rbcasp3 originated from a common ancestor of vertebrates, as indicated by the clustering pattern of mammals, avians and amphibians in their relevant clades. However, caspase 3A from Japanese Medaka formed an out group with the other clustered fish species, showing a distant relationship with other caspases 3 counterparts from fish, considered in the analysis.

3.2. Genomic structure and promoter analysis of Rbcasp3

The full-length *Rbcasp3* gDNA is 7529 bp in length and consists of six exons interrupted by five introns. (GenBank ID: JQ315116; Fig. 4). The sequence around the exon/intron boundaries follows the AG-GT rule, which is generally important in splicing processes. The characterized gDNA sequence was compared with four previously characterized gDNA sequences of fish and human (obtained from the Ensemble genome site, (www.ensembl.org) (Fig. 4). According to the comparison, Rbcasp3 gene and caspase 3 from sea bass [17] and fugu (Ensemble ID: SINFRUT00000160403) have similar patterns of exon–intron organization, whereas the size of their introns varies considerably. The human caspase 3 gene (Ensemble ID: ENSDART00000005593) contains relatively long exons, as compared to caspase 3 in the other four organisms examined. However the characteristic common feature that is present in all five caspase 3 genes is the intron-interruption of the penta-peptide active site motif (QACRG) after its first amino acid. The sequence upstream of the *Rbcasp3* transcription initiation site was analyzed and results revealed a number of potential *cis* elements, most of them are similar to those identified from previous promoter studies of other caspase 3 homologs [35,36] (Fig. 5).

3.3. Tertiary structural model of Rbcasp3

In order to determine the tertiary structure of pro-caspase 3 of rock bream, 3D modeling was conducted using the I-TASSER ab-initio protein prediction algorithm. The top ten caspase template crystal structures from the Research Collaboratory for Structural Bioinformatics (RCSB) protein data bank used by the server exhibited over 56% identity in the threading-aligned region, with the query sequence and the Z-score values of the threading alignments exceeding 1, which ensured a considerable reliability of the predicted structure. The predicted 3D model of Rbcasp3 consisted of 5 α-helices, 21 β-strands, and 31 turns. The large and small domains, along with the linker region, resembled the typical

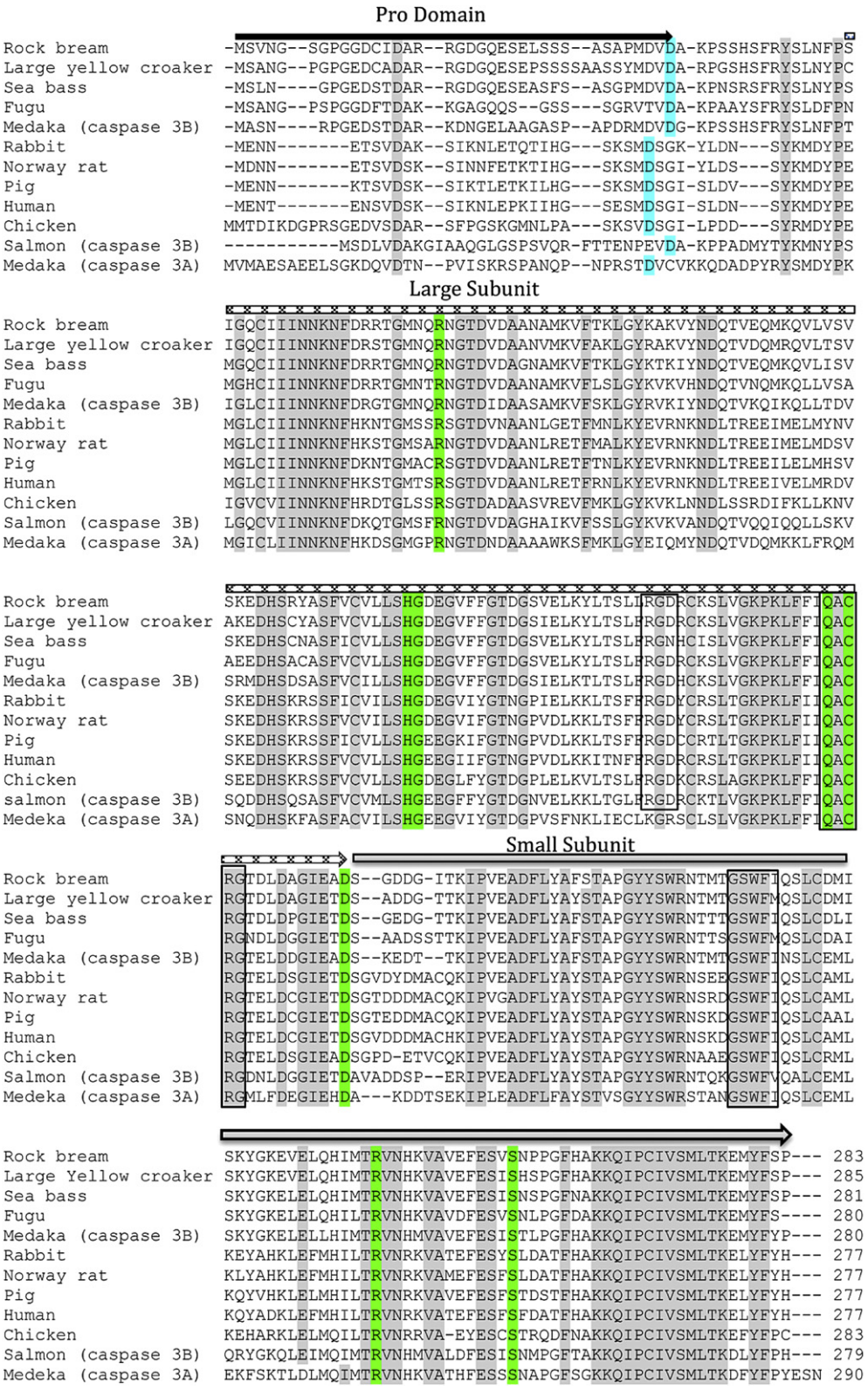

Fig. 2. Multiple sequence alignment of vertebrate caspase 3. Sequence alignments were obtained by the ClustalW method. Conserved residues are shaded in gray. The putative cleavage sites at aspartic acid residues, where the separation of relevant domains occurs, are indicated by pale blue shading. Several critical residues in the caspase 3 catalytic center and binding pocket are indicated by pale green shading. The protein binding domain (GSWFI), the integrin recognition motif (RGD), and the penta-peptide active site motif (QACRG) are indicated by boxes. (For interpretation of the references to colour in this figure legend, the reader is referred to the web version of this article.)

caspase 3 structure [37], comprising a central hexa-stranded β-sheet with five parallel and one anti-parallel strands, a double-stranded anti-parallel β-sheet at the top of the structure, and another double-stranded anti-parallel β-sheet at the front of the molecule. Moreover, there are five helices, three on one side of the main hexa-stranded β-sheet and two on the opposite side (Fig. 6).

Table 2
Percent identities of Rbcasp3 gene with caspase 3 genes from other species.

Common name	Protein	Accession number	Identity (%)
Large yellow croaker	Caspase 3	ACJ65025	88.8
European seabass	Caspase 3	ABC70996	88.0
Fugu rubripes	Caspase 3	AAM43816	80.3
Atlantic salmon	Caspase 3 precursor	ACN11423	79.9
Japanese Medaka	Caspase 3B	NP001098168	78.3
Zebrafish	Caspase 3	CAX14649	73.0
White cloud mountain minnow	Caspase 3	ACV31395	72.8
Atlantic salmon	Caspase 3	NP001133393	62.8
Northern pike	Caspase 3 precursor	ACO13502	61.7
Chicken	Caspase 3	AAC32602	59.2
Rabbit	Caspase 3 precursor	NP001075586	57.0
Pig	Caspase 3 precursor	NP999296277	56.7
Norway rat	Caspase 3	NP037054	55.4
Human	Caspase 3 preproprotein	NP116786	54.1
House mouse	Caspase 3	NP033940, XP996914	53.8
African clawed frog	Caspase 3 -precursor	NP001081226	52.0
Blood fluke	Caspase 3	ACU88129	34.7
Southern house mosquito	Caspase 3	XP001850595	32.7
Fruit fly	Death executioner caspase related to Apopain	AAF55329	30.0
Black tiger shrimp	Caspase 3	ADV17345	28.4

3.4. Recombinant expression and purification of Rbcasp3

Rbcasp3, without the pro-domain, was sub-cloned into the pMAL-c2X vector and overexpressed under the strong tac promoter as a fusion protein with MBP in *E. coli* BL21 (DE3) cells by IPTG-driven induction. Fractions collected at different stages during the purification process of the expressed protein were visualized by SDS-PAGE (Fig. 7). The molecular mass of the purified rRbcasp3 was visually determined to be ~74 kDa, appeared as a single band. This result was compatible with the predicted molecular mass of the putative caspase 3 (~31 kDa), since the molecular mass of the MBP was around 42.5 kDa.

3.5. Hydrolyzing activity of Rbcasp3

To confirm the hydrolyzing activity of the Rbcasp3, the purified fusion protein was employed to hydrolyze the caspase 3/7-specific synthetic substrate, DEVD-*p*NA, along with the control MBP. Compared to MBP (mean A_{400}:−0.05), rRbcasp3 exerted almost 12-fold more activity against the substrate (mean A_{400}:−0.63), suggesting the biochemical function of Rbcasp3 while indicating comparatively low activities, against caspases 9 substrate, LEHD-*p*NA (mean A_{400}:−0.31) and caspases 8 substrate, IETD- *p*NA (mean A_{400}:−0.28) (Fig. 8).

3.6. Analysis of the tissue-specific expression profile of Rbcasp3

In order to determine the tissue-specific Rbcasp3 transcription profile in normal rock bream, qRT-PCR was carried out on various rock bream tissues using gene specific primers designed according to the *Rbcasp3* full-length cDNA sequence. The relative expression of each tissue was obtained by comparison to expression of the rock bream β-actin gene, which was used as the non-variant internal control. To determine relative levels of tissue-specific expression, β-actin-normalized expression of each tissue was further normalized to that in the muscle (Fig. 9). Rbcasp3 mRNA was found to be constitutively expressed in all tissues investigated.

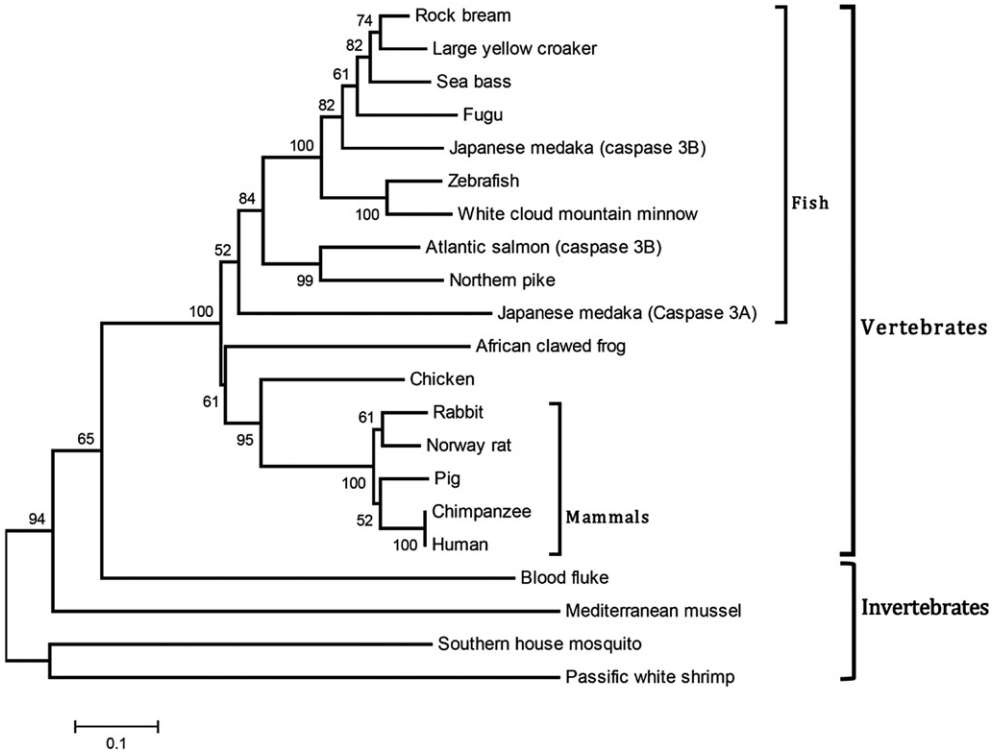

Fig. 3. Phylogenetic analysis of Rbcasp3. The tree constructed based on ClustalW alignment of deduced amino acid sequences of various caspase 3 proteins, estimated by the Neighbor-Joining method in MEGA version 4.0. Bootstrap values are shown for each of the lineages of the tree, and major taxonomic clusters are indicated within parentheses.

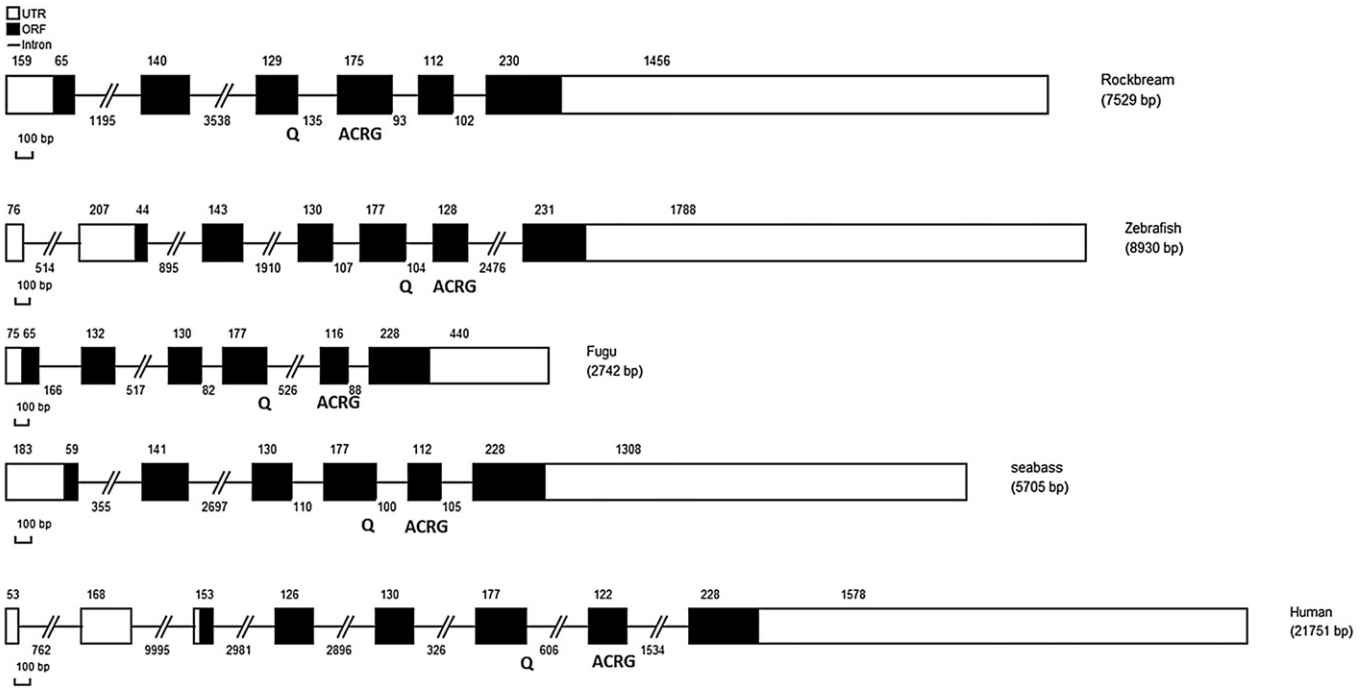

Fig. 4. Genomic organization of the caspase 3 genes from rock bream, zebrafish, fugu, sea bass and human. The exons are represented by boxes and introns by solid lines. The sizes of exons are indicted above the exons and sizes of introns are indicated below the introns. Sequence regions larger than 300 bp are truncated by two inclined lines. (Sequence direction – 5′ → 3′).

However, a distinct tissue-specific transcriptional profile was found, in which the *Rbcasp3* transcription levels were highest in blood, moderately high ($P < 0.05$) in liver, heart and brain tissues, and considerably low ($P < 0.05$) in all other tissues analyzed (Fig. 9).

3.7. Transcriptional responses of Rbcasp3 upon immune challenges

Liver tissue from LPS, poly(I:C), iridovirus and *E. tarda* challenged rock bream was used to analyze the mRNA expression levels in response to immune stimulations. The qRT-PCR detected *Rbcasp3* expression levels were normalized to the rock bream β-actin expression profile and compared to the transcript level detected in PBS-injected controls at each time point.

In liver cells of LPS-challenged fish, the *Rbcasp3* transcript levels were significantly ($P < 0.05$) up-regulated at 12 h and 24 h post-injection, indicating ~2.5 fold expression increase at both time points (Fig. 10A). In contrast, liver cells of the *E. tarda*-challenged animals exhibited a significant ($P < 0.05$) and persistent up-regulation from 3 h to 48 h post-injection, reaching peak expression (3-fold) at 48 h. However, at all the time points examined, the transcription was induced by *E. tarda* with respect to the basal level (0 h), (Fig. 10A).

As shown in the Fig. 10B, at 3 h and 6 h after poly(I:C) injection, the *Rbcasp3* transcription profile in liver cells exhibited a significant early-phase increase ($P < 0.05$) with the peak (2.6-fold) occurring at the 6 h time point. However, a subsequent down-regulation was observed at 24 h post-injection, followed by a significant late-phase increase (2.4-fold, $P < 0.05$) at 48 h post-injection. Fig. 10B also depicts the differential mRNA expression profile of Rbcasp3 in liver tissue in response to the RBIV challenge. Over the experiment time course, the Rbcasp3 expression slightly fluctuated up to 24 h post-injection, followed by a significant increase (3.3-fold) at 48 h, which indicated the late-phase response to the viral-induced immune challenge.

4. Discussion

Apoptosis can play a key role in defense of an organism through limiting the pool of host cells for the productive replication of pathogenic organisms such as bacteria and viruses [38]. Caspase 3 is a pivotal regulator of the executionary phase of apoptosis, and is involved in many of the molecular mechanisms underlying programmed cell death [39]. Therefore, the elevated activity of caspase 3 can be considered as a useful bio-marker of cells undergoing apoptosis [40]. However, information on caspase 3 in fish at the genomic level is relatively scarce. In the present study, the caspase 3 gene was identified in rock bream and characterized structurally and functionally. The rock bream species is an important member of the marine aquaculture industries in countries located in the Asia-Pacific zone. To gain a better understanding of how rock bream immunity may be modulated, transcriptional responses of the newly-identified caspase 3 homolog toward several common pathogenic microorganisms were investigated. The putative caspase 3 gene was identified from our previously established (GS-FLX™) rock bream cDNA sequence database by using BLAST analysis. This novel gene was found to exhibit 88.8% identity with the caspase 3 gene from large yellow croaker (Table 2). Moreover, the ORF (283 aa) and the predicted molecular mass of deduced amino acids of Rbcasp3 showed a higher similarity to caspase 3 molecules of other fish species and its mammalian counterparts [17–19,41,42]. The presence of characteristic domain organization (pro-domain, large subunit, and small subunit) and the predominant features of caspase family signatures, such as the penta-peptide binding motif, the protein binding domain (GSWFI), RGD motif, and critical amino acid residues in the catalytic center and binding pocket lent credence to the hypothesis that Rbcasp3 was indeed a caspase 3 homolog (Fig. 2).

The predicted genomic structure of Rbcasp3 shares similar intron/exon architecture with the caspase 3 homologs in a majority of fish species (Fig. 4). However the genome structure deviates from that in the zebrafish (Ensemble ID: ENSDART00000005593), which has one

Fig. 5. Deduced promoter region of Rbcasp3. The transcription initiation site (+1) is denoted by a curved arrow. Putative transcription factor binding sites predicted by the TFSEARCH and Alibaba 2.1 programs are indicated by bold letters with their corresponding identity. The SRY site starts from position −417 in the sequence and is in complement form in the reverse direction.

more exon. This additional exon in zebrafish contains a part of the 5′-UTR, altogether using two exons for the complete 5′-UTR, and more closely resembling the human caspase 3 genomic structure (Ensemble ID: ENST00000308394). The length of each exon in rock bream caspase 3 is almost identical to the corresponding exons in sea bass, even though the gene arrangements are different with respect

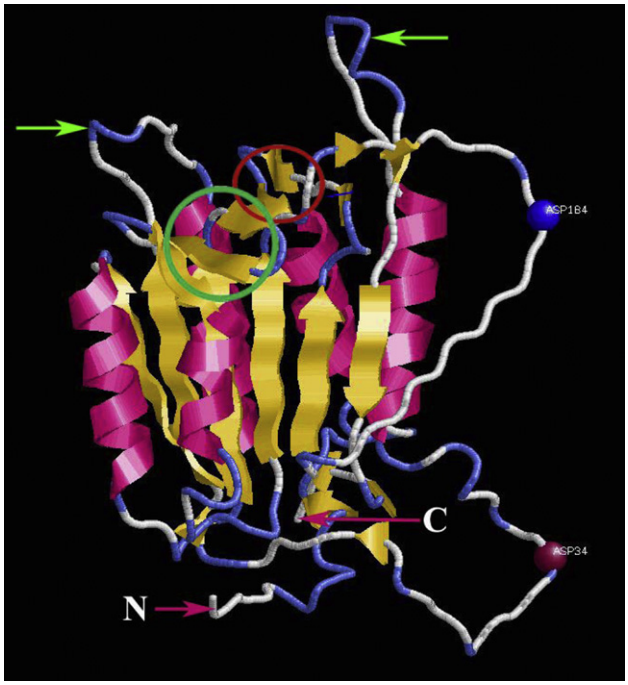

Fig. 6. Predicted 3D structural model of rock bream pro-caspase 3. Two spherical bulges (Asp 34, and Asp 184) represent the two aspartate residues where the pro-domain and the large domain is cleaved off, respectively. Green arrows indicate the two characteristic extra loops of caspase 3 architecture. β-strands are depicted in yellow and α-helices are in pink. Turns are represented in blue in the back-bone structure. Two anti-parallel double-stranded β-sheets are encircled in red and green color. The letters C and N indicate the carboxyl and amino terminals, respectively. (For interpretation of the references to colour in this figure legend, the reader is referred to the web version of this article.)

to their intron lengths. Interestingly, the conserved penta-peptide binding motif is interrupted by an intron after its first amino acid in all the species, serving as a unique feature of caspase 3 genome organizations.

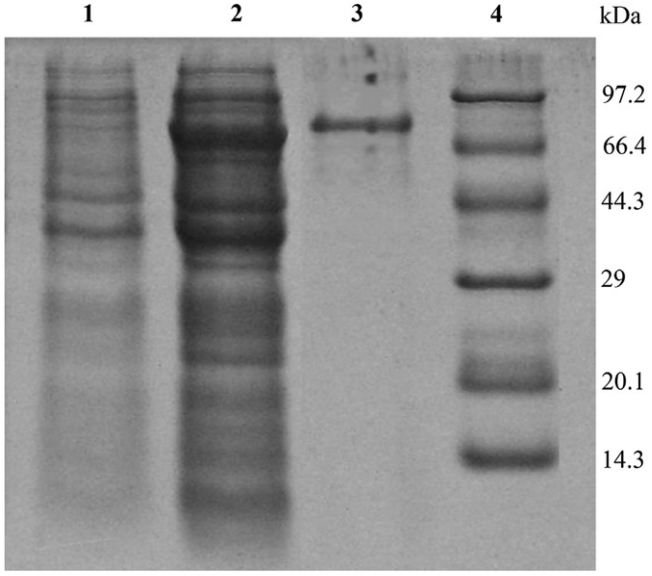

Fig. 7. SDS-PAGE analysis of overexpressed and purified recombinant Rbcasp3 fusion protein. Lane 1, total cellular extract from *E. coli* BL21 (DE3) carrying the Rbcasp3-MBP expression vector prior to IPTG induction; 2, crude extract of rRbcasp3; 3, purified recombinant fusion protein (rRbcasp3-MBP) after IPTG induction (1 mM); 4, protein markers (TaKaRa).

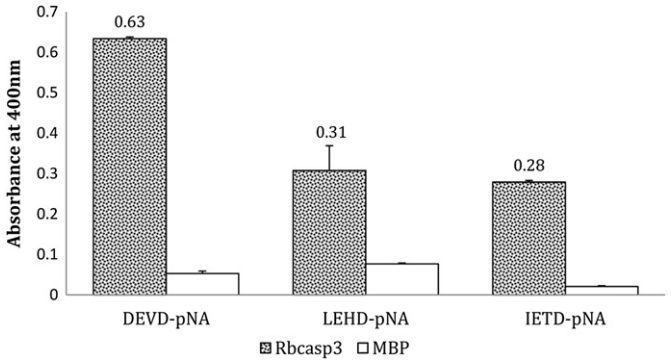

Fig. 8. *In vitro* Rbcasp3 hydrolyzing activity assay. The hydrolyzing activity against DEVD-*p*NA is represented using the corresponding absorbance value obtained at 400 nm. Error bars represent the SD ($n = 3$).

The predicted promoter region of *Rbcasp3* was determined to consist of ~1 Kb sequence, which includes several putative transcription factor binding sites (Fig. 5), substantiating the notion of tight regulation of caspase gene expression. Particularly, the putative transcription factor binding sites that were identified are known to be involved in transcriptional activation (GCN4 motif) [43], LPS-induced signaling (AP-1) [44], virus-induced cell signaling (OCT-1) [45], and oncogenic transcriptional activation (Pbx-1) [46]. Presence of the latter three sites suggested that the anticipated promoter region, which presumably drives the transcription of *Rbcasp3* may be activated by different immune stimulants, as well as neoplastic signals.

Phylogenetic analysis of Rbcasp3 indicated that fish and mammalian sub-clusters are independently clustered into a vertebrate clade (Fig. 3). Furthermore the tree revealed that Rbcasp3 is evolutionarily more close to caspase 3B isoform from Japanese Medaka and Atlantic salmon, rather than caspase 3A isoform from Medaka, providing evidence to propose that the identified and cloned novel Rbcasp3 may be the variant B of caspases 3 in rock bream. In addition, clustering pattern indicated that caspase 3 from southern house mosquito and pacific white shrimp share a common ancestor, supporting the close evolutionary relationship of caspase 3 in insects and crustaceans.

Our computational-based attempt to determine the tertiary structure of rock bream pro-caspase 3 (Fig. 6) generated the distinctive caspase 3 structure, with regard to the known large and small domains of human caspase 3 [42]. As described in the results section, the 3D model was comprised of corresponding β-sheets, α-helices, and extra loops with respect to the relevant positions, corroborating the existence of the novel rock bream pro-caspase 3.

Caspases are known to be active as tetramers, consisting of large and small subunit heterodimers, after proteolysis. Furthermore, this proteolysis can be occurred through auto activation, trans-activation or by other proteinases. However in previous studies, it was demonstrated that caspases can show low, but detectable activity as non-processed pro-enzymes [47] According to the SDS-PAGE analysis, purified rRbcasp3 was appeared as a single band, directing us to conclude that after purification, the recombinant caspases 3 has not been auto-processed.

The hydrolyzing activity assay with rRbcasp3 fusion protein showed a substantial activity relative to the control MBP, against the mammalian caspase 3/7-specific substrate, DEVD-*p*NA (Fig. 8). This finding indicated that Rbcasp3 harbors the typical biochemical property of caspase 3, affirming the functional similarly of Rbcasp3 with known members of the caspase 3 subfamily. Moreover, compared to the activity detected against caspases 9 (LEHD-*p*NA) and caspase 8 substrate (IETD-*p*NA), Rbcasp3 exerted a noticeable

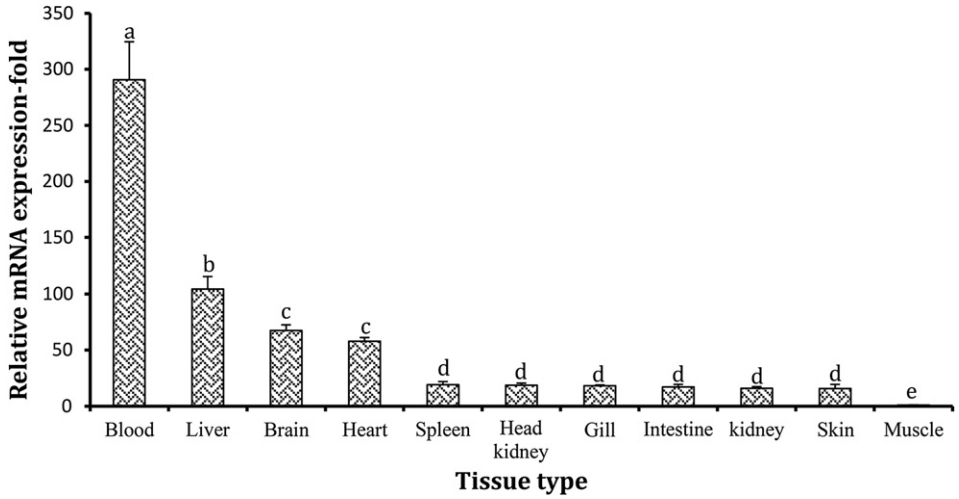

Fig. 9. Tissue expression analysis of *Rbcasp3* mRNA, as determined by qRT-PCR. Error bars represent the SD ($n = 3$). Data with different letters are significantly different ($P < 0.05$) among different tissues.

specificity against caspase 3/7 substrate, DEVD-*p*NA (Fig. 8). However, low but detectable activity; exerted by Rbcasp3 against non caspases 3/7 substrates may be attributed with multi-substrate tolerable property of caspases 3 molecules, in certain extend [48].

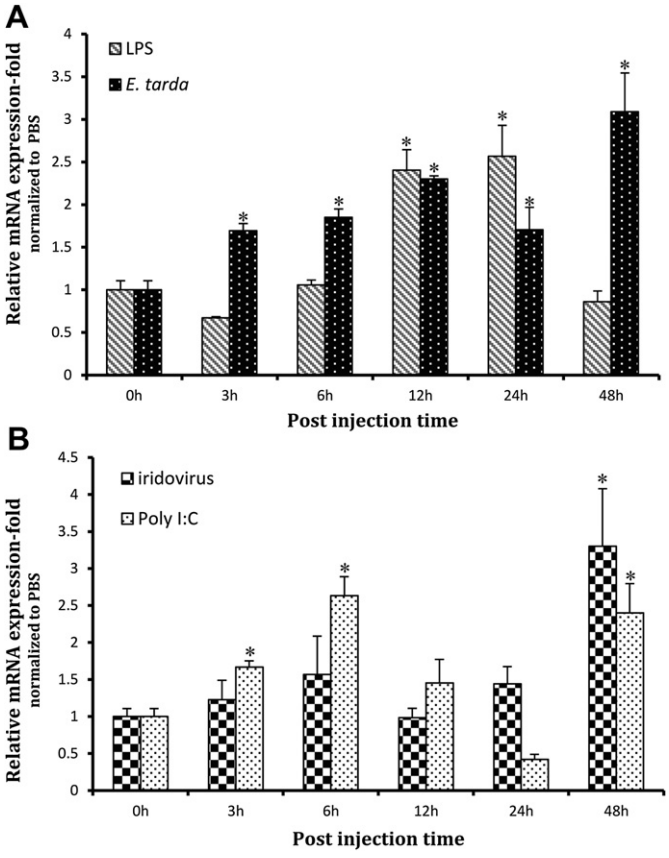

Fig. 10. Expression profile of *Rbcasp3* mRNA in liver tissue upon immune stimulation with (A) LPS or *E. tarda* bacteria, (B) poly(I:C) or iridovirus, as determined by qRT-PCR. The relative expression was calculated by the $2^{-\Delta\Delta CT}$ method using rock bream β-actin as the reference gene with respect to corresponding PBS-injected controls at each time point. The relative expression fold-change at 0 h post-injection was used as the basal line. Error bars represent the SD ($n = 3$), $^{*}P < 0.05$.

According to the qRT-PCR analysis, caspase 3 transcripts were detectable in every rock bream tissue tested, to varying degree (Fig. 9). The highest expression level was detected in blood, whereas the lowest was detected in muscle. This pattern was in agreement with that shown in a previous study of caspase 3 in large yellow croaker [19]. Similarly, the rock bream expression pattern was consistent with that in sea bass, whereby moderately higher transcription level was observed in heart and relatively low levels were detected in spleen, intestine, and head kidney [17]. However, in rock bream, the second most abundant expression of caspase 3 was detected in liver, which is a potent immune-related organ involved in host defense [49,50], although it was found to be much lower in sea bass and large yellow croaker [17,19]. In mammalian tissues, caspase 3 mRNA expression is more or less compatible with the expression patterns reported for fish. Evaluation of mRNA expression of rat caspase 3 exhibited an omnipresent expression in every tissue tested, with remarkably predominant levels in spleen, kidney, thymus and lung [51]. Moreover, mouse caspase 3 transcripts were abundantly detected in spleen, but scarcely detected in brain, lung, liver, and kidney [51]. Hence, the ubiquitous expression of caspase 3 mRNA in various immune-related tissues of different organisms supports the notion that caspase 3 can play a significant role in host immunity.

In order to investigate the potential of apoptosis in rock bream liver tissues as an immune-related responses to viral and bacterial infections, Rbcasp3 gene expression was evaluated by qRT-PCR during challenges with *E. tarda*, a gram-negative bacteria, and LPS, a well-characterized endotoxin in the cell wall of gram-negative bacteria as well as with iridovirus, a virulent pathogen of rock bream, and poly(I:C), a pathogen-associated molecular pattern (PAMP) that emulates the double-stranded viral DNA. The transcriptional response to *E. tarda* challenge revealed that *Rbcasp3* is a candidate gene for bacterial induction. At all the time points between 3 h and 48 h post-injection, *Rbcasp3* was significantly up-regulated reaching its peak at 48 h (Fig. 10A). This observation is in agreement with the induction pattern reported for sea bass upon *phdp* stimulation [17] and that detected during trivalent bacterial vaccine challenge in large yellow croaker [19]. However, in our LPS challenge, significant *Rbcasp3* up-regulation was only noticed at two time points: 12 h and 24 h post-injection, which would be considered late-responses, as compared to *E. tarda* induction. This may due to the different forms of the bacterial stimulants used in both experiments. Since *E. tarda* is a live pathogenic bacterium, it

can instigate a relatively strong immune response, as compared to LPS injection, which is a nonliving chemical component isolated from the bacterial cell wall. According to the viral challenges, Rbcasp3 exhibited significant up-regulation in response to both poly(I:C) and iridovirus. The poly(I:C) elicited a rapid response (3 h and 6 h post-injection) (Fig. 10B). The difference in the above two responses may be attributed to the different PAMP markers inducing corresponding receptors on the host immune cells. Altogether, these results suggest that temporal transcriptional modulations of caspase 3 in rock bream, involved in apoptotic cascade, can be triggered by bacterial and viral infections.

In summary, the full-length cDNA and the genomic DNA sequences of rock bream caspase 3 gene were identified from the previously established cDNA and genomic DNA libraries, respectively. Structural and functional characterization was carried out, along with analysis of the transcriptional variations in healthy and immune-challenged fish. Phylogenetic analysis revealed the prominent evolutionary relationships of Rbcasp3 with other vertebrate species, especially with fish. Bioinformatics analysis of the predicted promoter region provided initial insights into the regulatory factors of Rbcasp3 expression. Moreover, recombinant caspase 3 protein displayed protease properties against its specific substrate, substantiating its functional viability. The immune response of Rbcasp3 gene expression upon viral and bacterial challenges provided evidence of the involvement of caspase 3 in viral and bacterial defense in rock bream. Future research investigating, the dynamic contribution of caspase 3 in rock bream may help to solve the pathogenic threat on the fish.

Acknowledgment

This research was supported by National Fisheries Research and Development Institute (RP-2012-BT-003) grant.

References

[1] Earnshaw WC, Martins LM, Kaufmann SH. Mammalian caspases: structure, activation, substrates, and functions during apoptosis. Annu Rev Biochem 1999;68:383–424.
[2] Grütter MG. Caspases: key players in programmed cell death. Curr Opin Struct Biol 2000;10:649–55.
[3] Galluzzi L, Vitale I, Abrams JM, Alnemri ES, Baehrecke EH, Blagosklonny MV, et al. Molecular definitions of cell death subroutines: recommendations of the Nomenclature Committee on Cell Death 2012. Cell Death Differ 2012;19:107–20.
[4] Everett H, McFadden G. Apoptosis: an innate immune response to virus infection. Tren Micro Biol 1999;7:160–5.
[5] Sun EW, Shi YF. Apoptosis: the quiet death silences the immune system. Pharmacol Ther 2001;92:135–45.
[6] Thornberry NA, Lazebnik Y. Caspases: enemies within. Science 1998;281:1312–6.
[7] Cohen GM. Caspases: the executioners of apoptosis. Biochem J 1997;326:1–16.
[8] Nicholson DW. Caspase structure, proteolytic substrates, and function during apoptotic cell death. Cell Death Differ 1999;6:1028–42.
[9] Ganesan R, Mittl PR, Jelakovic S, Grütter MG. Extended substrate recognition in caspase-3 revealed by high resolution X-ray structure analysis. J Mol Biol 2006;359:1378–88.
[10] Nicholson DW, Thornberry NA. Caspases: killer proteases. Trends Biochem Sci 1997;22:299–306.
[11] Fuentes-Prior P, Salvesen GS. The protein structures that shape caspase activity, specificity, activation and inhibition. Biochem J 2004;1(384):201–32.
[12] Miao EA, Leaf IA, Treuting PM, Mao DP, Dors M, Sarkar A, et al. Caspase-1-induced pyroptosis is an innate immune effector mechanism against intracellular bacteria. Nat Immunol 2010;11:1136–42.
[13] Ho PK, Hawkins CJ. Mammalian initiator apoptotic caspases. FEBS J 2005;272:5436–53.
[14] Boyce M, Degterev A, Yuan J. Caspases: an ancient cellular sword of Damocles. Cell Death Differ 2004;11:29–37.
[15] Deveraux QL, Reed JC. IAP family proteins–suppressors of apoptosis. Genes Dev 1999;13:239–52.
[16] Lavrik IN, Golks A, Krammer PH. Caspases: pharmacological manipulation of cell death. J Clin Invest 2005;115:2665–72.
[17] Reis MI, Nascimento DS, do Vale A, Silva MT, dos Santos NM. Molecular cloning and characterisation of sea bass (*Dicentrarchus labrax* L.) caspase-3 gene. Mol Immunol 2007;44:774–83.
[18] Yabu T, Kishi S, Okazaki T, Yamashita M. Characterization of zebrafish caspase-3 and induction of apoptosis through ceramide generation in fish fathead minnow tailbud cells and zebrafish embryo. Biochem J 2001;360:39–47.
[19] Li M, Ding Y, Mu Y, Ao J, Chen X. Molecular cloning and characterization of caspase-3 in large yellow croaker (*Pseudosciaena crocea*). Fish Shellfish Immunol 2011;30:910–6.
[20] Takle H, McLeod A, Andersen O. Cloning and characterization of the executioner caspases 3, 6, 7 and Hsp70 in hyperthermic Atlantic salmon (*Salmo salar*) embryos. Comp Biochem Physiol B Biochem Mol Biol 2006;144:188–98.
[21] Naruse K, Fukamachi S, Mitani H, Kondo M, Matsuoka T, Kondo S, et al. A detailed linkage map of Medaka, Oryzias latipes: comparative genomics and genome evolution. Genetics 2000;154:1773–84.
[22] Zenke K, Kim KH. Functional characterization of the RNase III gene of rock bream iridovirus. Arch Virol 2008;153:1651–6.
[23] Park SL. Disease control in Korean aquaculture. Fish Pathol 2009;44:19–23.
[24] Whang I, Lee Y, Kim H, Jung SJ, Oh MJ, Choi CY, et al. Characterization and expression analysis of the myeloid differentiation factor 88 (MyD88) in rock bream *Oplegnathus fasciatus*. Mol Biol Rep 2011;38:3911–20.
[25] Tamura K, Dudley J, Nei M, Kumar S. MEGA4: Molecular Evolutionary Genetics Analysis (MEGA) software version 4.0. Mol Biol Evol 2007;24:1596–9.
[26] Reese MG. Application of a time-delay neural network to promoter annotation in the *Drosophila melanogaster* genome. Comput Chem 2001 Dec;26(1):51–6.
[27] Roy A, Kucukural A, Zhang YI. TASSER: a unified platform for automated protein structure and function prediction. Nat Protoc 2010;5:725–38.
[28] Zhang Y. I-TASSER server for protein 3D structure prediction. BMC Bioinform 2008;9:40.
[29] Umasuthan N, Whang I, Kim JO, Oh MJ, Jung SJ, Choi CY, et al. Rock bream (*Oplegnathus fasciatus*) serpin, protease nexin-1: transcriptional analysis and characterization of its antiprotease and anticoagulant activities. Dev Comp Immunol 2011;35:785–98.
[30] Bradford MM. A rapid and sensitive method for the quantitation of microgram quantities of protein utilizing the principle of protein-dye binding. Anal Biochem 1976;72:248–54.
[31] Whang I, Lee Y, Lee S, Oh MJ, Jung SJ, Choi CY, et al. Characterization and expression analysis of a goose-type lysozyme from the rock bream *Oplegnathus fasciatus*, and antimicrobial activity of its recombinant protein. Fish Shellfish Immunol 2011;30:532–42.
[32] Livak KJ, Schmittgen TD. Analysis of relative gene expression data using real-time quantitative PCR and the 2(-Delta Delta C(T)) Method. Methods 2001;25:402–8.
[33] Johnson AL, Bridgham JT. Caspase-3 and -6 expression and enzyme activity in hen granulosa cells. Biol Reprod 2000;62:589–98.
[34] Pierschbacher MD, Ruoslahti E. Cell attachment activity of fibronectin can be duplicated by small synthetic fragments of the molecule. Nature 1984;309:30–3.
[35] Liu W, Wang G, Yakovlev AG. Identification and functional analysis of the rat caspase-3 gene promoter. J Biol Chem 2002;277:8273–8.
[36] Liedtke C, Groger N, Manns MP, Trautwein C. The human caspase-8 promoter sustains basal activity through SP1 and ETS-like transcription factors and can be up-regulated by a p53-dependent mechanism. J Biol Chem 2003;278:27593–604.
[37] Rotonda J, Nicholson DW, Fazil KM, Gallant M, Gareau Y, Labelle M, et al. The three-dimensional structure of apopain/CPP32, a key mediator of apoptosis. Nat Struct Biol 1996;3:619–25.
[38] Chang HY, Yang X. Proteases for cell suicide: functions and regulation of caspases. Microbiol Mol Biol Rev 2000;64:821–46.
[39] Gerald M. Caspases: the executioners of apoptosis. Biochem J Rev 1997;326:1–16.
[40] Abu-Qare AW, Abou-Donia MB. Biomarkers of apoptosis: release of cytochrome c, activation of caspase-3, induction of 8-hydroxy-2'-deoxyguanosine, increased 3-nitrotyrosine, and alteration of p53 gene. J Toxicol Environ Health B Crit Rev 2001;4:313–32.
[41] Wang H, Keiser JA. Molecular characterization of rabbit CPP32 and its function in vascular smooth muscle cell apoptosis. Am J Physiol 1998;274:1132–40.
[42] Fernandes-Alnemri T, Litwack G, Alnemri ES. CPP32, a novel human apoptotic protein with homology to Caenorhabditis elegans cell death protein Ced-3 and mammalian interleukin-1 beta-converting enzyme. J Biol Chem 1994;269:30761–4.
[43] Hope IA, Struhl K. GCN4, a eukaryotic transcriptional activator protein, binds as a dimer to target DNA. EMBO J 1987;6:2781–4.
[44] Guha M, Mackman N. LPS induction of gene expression in human monocytes. Cell Signal 2001;13:85–94.
[45] Lee L, Stollar E, Chang J, Grossmann JG, O'Brien R, Ladbury J, et al. Expression of the Oct-1 transcription factor and characterization of its interactions with the Bob1 coactivator. Biochemistry 2001;40:6580–8.
[46] Mazieres J, You L, He B, Xu Z, Lee AY, Mikami I, et al. Inhibition of Wnt16 in human acute lymphoblastoid leukemia cells containing the translocation induces apoptosis. Oncogene 2005;24:5396–400.

[47] Wolf BB, Green DR. Suicidal tendencies: apoptotic cell death by caspase family proteinases. J Biol Chem 1999;274:20049–52.
[48] Fang B, Boross PI, Tozser J, Weber IT. Structural and kinetic analysis of caspase-3 reveals role for s5 binding site in substrate recognition. J Mol Biol 2006;360:654–66.
[49] Seki S, Habu Y, Kawamura T, Takeda K, Dobashi H, Ohkawa T, et al. The liver as a crucial organ in the first line of host defense: the roles of Kupffer cells, natural killer (NK) cells and NK1.1 Ag+ T cells in T helper 1 immune responses. Immunol Rev 2000;174:35–46.
[50] Sheth K, Bankey P. The liver as an immune organ. Curr Opin Crit Care 2001;7:99–104.
[51] Juan TS, McNiece IK, Jenkins NA, Gilbert DJ, Copeland NG, Fletcher FA. Molecular characterization of mouse and rat CPP32 beta gene encoding a cysteine protease resembling interleukin-1 beta converting enzyme and CED-3. Oncogene 1996;13:749–55.